


**Please cite the Published Version**

Hurst, G, Ruiz-Lopez, S, Rivett, D and Tedesco, S  (2022) Effect of hydrochar from acid hydrolysis on anaerobic digestion of chicken manure. Journal of Environmental Chemical Engineering, 10 (5). 108343 ISSN 2213-3437

**DOI:** <https://doi.org/10.1016/j.jece.2022.108343>

**Publisher:** Elsevier

**Version:** Published Version

**Downloaded from:** <https://e-space.mmu.ac.uk/630231/>

**Usage rights:**  [Creative Commons: Attribution 4.0](https://creativecommons.org/licenses/by/4.0/)

**Additional Information:** This is an Open Access article which appeared in Journal of Environmental Chemical Engineering, published by Elsevier

**Data Access Statement:** Data will be made available on request.

**Enquiries:**

If you have questions about this document, contact [openresearch@mmu.ac.uk](mailto:openresearch@mmu.ac.uk). Please include the URL of the record in e-space. If you believe that your, or a third party's rights have been compromised through this document please see our Take Down policy (available from <https://www.mmu.ac.uk/library/using-the-library/policies-and-guidelines>)



# Effect of hydrochar from acid hydrolysis on anaerobic digestion of chicken manure

G. Hurst<sup>a,\*</sup>, S. Ruiz-Lopez<sup>b</sup>, D. Rivett<sup>b</sup>, S. Tedesco<sup>a,c,\*</sup>

<sup>a</sup> Department of Engineering, Manchester Metropolitan University, Dalton Building, Chester Street, Manchester M1 5GD, UK

<sup>b</sup> Department of Natural Sciences, School of Science and the Environment, Manchester Metropolitan University, Dalton Building, Chester Street, Manchester M1 5GD, UK

<sup>c</sup> Advanced Materials and Surface Engineering (AMSE) Research Centre, Manchester Metropolitan University, Dalton Building, Chester Street, Manchester M1 5GD, UK

## ARTICLE INFO

### Keywords:

Acid hydrolysis  
Levulinic acid  
Hydrochar  
Anaerobic digestion  
Chicken manure  
Microbial assay

## ABSTRACT

Acid hydrolysis is a key process for the production of platform chemicals from biomass, however solid residues by-products can amount to 50 wt% of the starting biomass material. In this study, solid residues from the production of biofuel precursor levulinic acid were generated via microwave-assisted acid hydrolysis of *Miscanthus x Giganteus* and investigated for the supplementation of anaerobic reactors digesting Chicken Manure. The addition of the solid residues increased the methane yields by up to 14.1%, depending on the additive concentration levels, 2–10 g/L. A mild ammonium related inhibition was observed during the fermentation trials, which was mitigated by the solid residue additive. An experimental optimum of concentration 6 g/L residue was found which corresponded with a 20% decrease in ammonium concentrations and increased microbial diversity, where phyla Bacteroidetes and Firmicutes were the most prevalent, whilst the relative abundance of Archaea (Euryarchaeota) decreased without negative effects on methane production. The effects of acid catalysis conditions on solid residue properties and methane yields from chicken manure were evaluated. All solids residue investigated exhibited ammonium absorption and improved microbial diversity during anaerobic digestion. The integration of anaerobic digestion downstream second generation biorefineries is a promising green waste disposal method for solid by-products from thermo-catalytic processes.

## 1. Introduction

The establishment of bio-based industries is necessary for the transition to a low carbon economy. Second generation biorefineries can convert lignocellulosic biomass into a spectrum of bio-products through multitude thermochemical processes, such as aqueous catalysis, gasification, pyrolysis and ionic liquids. Acid-catalysed hydrolysis operates at relatively mild temperatures (150–250 °C) and is considered a promising approach for the production of key platform chemicals, including levulinic acid (LA), furfural and 5-hydroxymethylfurfural (5-HMF) [1,2]. Acid catalysed hydrolysis processes have many advantages including high selectivity, lower utility costs and relatively fast reaction times [3]. Several commercial-scale plants have been developed (e.g. Biofine and GFBiochemicals) to produce LA and 5-HMF from biomass using mineral acids [4,5]. LA is an especially promising commodity chemical that can be transformed into a range of bio-materials including green solvents, plasticisers and textiles [6]. However, full commercial deployment has so far proven challenging.

Solid Residue (SR) by-product from acid hydrolysis is a significant unvalorised waste stream, which is primarily composed of lignin and hydrolysis-recalcitrant lignocellulose fractions, as well as condensation products from the degradation of reactive intermediaries [7,8]. The formation of solid degradation products (also referred to as humins in literature), has been attributed to dehydration of sugars and subsequent condensation polymerisation to form furan-rich carbonaceous solids [9, 10]. The optimization of LA production inherently results in humin yields, however humins have become to be regarded as an unavoidable carbonaceous by-product [11].

Moreover, the growth of bio-refining applications will require development of new processes to valorise all associated by-products, in-order to maximise the full potential of the raw biomass feedstock and improve commercial viability. Several applications for SR from biorefineries have been investigated in recent years including integrated biorefineries that have sought to use the SR as a combustion fuel. However, having these similar elemental composition to coal, they will result in high carbon emissions [12]. SR has also been utilised as;

\* Correspondence to: Department of Engineering, Manchester Metropolitan University, Manchester, UK.

E-mail addresses: [George.hurst2@stu.mmu.ac.uk](mailto:George.hurst2@stu.mmu.ac.uk) (G. Hurst), [s.tedesco@mmu.ac.uk](mailto:s.tedesco@mmu.ac.uk) (S. Tedesco).

<https://doi.org/10.1016/j.jece.2022.108343>

Received 4 April 2022; Received in revised form 17 June 2022; Accepted 25 July 2022

Available online 27 July 2022

2213-3437/© 2022 The Authors. Published by Elsevier Ltd. This is an open access article under the CC BY license (<http://creativecommons.org/licenses/by/4.0/>).

pyrolysis feedstock for the production of bio-liquids [13], a low carbon building material and also as a heterogeneous catalyst [14]. Similarities between SR from acid hydrolysis and hydrochar produced from hydrothermal carbonisation (HTC) have been found with red seaweed [15]. Hydrochars are carbonaceous residues formed during HTC of biomass in catalyst free aqueous conditions, which have been reported for high sorption properties and carbon sequestration potential [16]. Shi et al. [17] found similarities between hydrochar formation mechanisms to humins from acid hydrolysis via aldol-condensation/tautomerization, and suggested that furan-rich humin structures, formed under acidic condition, are an intermediate step of hydrochar formation [17]. Due to similar formation mechanism, both SR from acid hydrolysis and hydrochar may result in analogous material properties and potential applications.

The supplementation of anaerobic digesters with carbonaceous materials, including hydrochars and biochars, to increase methane yields by inhibitor absorption and support for microbial growth has become a burgeoning field of research [18–20]. AD is a widely used low-cost disposal process for organic matter as well as a source renewable energy in the form of biogas [21]. AD inhibition has been reported when high concentrations of inhibitors such as ammonia, fatty acids, furans, heavy metals and organic compounds, disrupt and destabilise the complex microbial community [22–24]. Inhibitory compounds can directly or indirectly destabilise AD and reduce methane yields. Chars have been reported to reduce aqueous concentrations of ammonia and metals ions, with notably improved methane yields [25]. This is especially applicable to the degradation of nitrogen-rich animal manures, which have been highlighted by several authors as a growing environmental concern. The addition of biochar and hydrochar have both been observed to improve methane yields from manures by +17% to +500% from the digestion of nitrogen rich feedstock's [26]. Another benefit of char addition is it can act as a form carbon sequestration [27]. However, the energy consumption and subsequent costs of carbonaceous material production has been so far a limiting factor [28]. As SR from acid hydrolysis is an inherent waste stream of lignocellulosic biorefineries, it could potentially be utilised as a large-scale low-cost supplement in AD digesters. However, the effects of acid hydrolysis SR as additive in AD systems are not well known.

The aim of this study is to investigate the addition of residual solids from acid hydrolysis on the anaerobic digestion of Chicken Manure (CM). Several SRs were co-produced alongside LA, using different acid hydrolysis reaction conditions of *Miscanthus x Giganteus* feedstock, with sulphuric acid as the catalyst, in microwave heated reactors. Increasing SR concentrations were added in batch AD reactors for the digestion of ammonia-rich CM. The effects of SR loadings on methane yields were experimentally modelled and determined using the modified Gompertz equation, in conjunction with readings of detected ammonium concentrations. The effects of the different acid hydrolysis reaction conditions on the SR structural and compositional properties have also been examined and discussed. Microbiome analysis of each AD reactor was also conducted to understand the effects of SR on AD microbial cell count, diversity and composition.

## 2. Methods

### 2.1. Inoculum seed and substrate composition

The inoculum used in the experiments was collected from a mesophilic ( $31 \pm 1$  °C) in two stages seven months apart, denominated Trial 1 and 2 from an industrial brewery anaerobic digester.

There was a significant performance change in biogas production during degasification between the two trials, hence each inoculum's composition has been reported in Table 1, which includes characterisation results of CM substrate. CM was collected, dried and stored in a desiccator to maintain consistency.

**Table 1**

Proximate and elemental characterisation of Inoculum and CM feedstock.

	CM	Inoculum Trial 1	Inoculum Trial 2
TS (% wt%)	87.7 ± 0.3	7.6 ± 0.8	9.0 ± 0.1
VS (% wt%)	64.7 ± 0.2	5.5 ± 0.6	7.0 ± 0.1
VS (%)	73.7 ± 0.4	72.1 ± 0.5	78.2 ± 1.1
pH	N/A	7.78	7.00
Ammonia (g/L)	N/A	1.10	0.94
C (% TS basis)	34.7	32.1	38.0
H (% TS basis)	5.2	4.7	5.9
N (% TS basis)	7.7	7.2	8.1
S (% TS basis)	0.8	0.9	0.8
O (% TS basis)	23.8	27.1	25.3

### 2.2. Preparation of solid residues

Oven dried *Miscanthus x Giganteus* (<0.2 mm particle size) was subjected to acid hydrolysis conditions with 2 M sulphuric acid catalyst using a microwave CEM 5 reactor. Post reaction, the aqueous phase was sampled and the solid residue was separated using 2 µm filter paper and washed with deionised water, before drying at 60 °C for 24 hrs. SR was stored in airtight containers before further characterisation and use during AD.

The reaction conditions were chosen from pilot data, (fixed solid-to-medium ratio of 5 wt%) to produce a diverse range of SR properties with consideration to high achieving LA yields, shown in Table 2. The highest LA yield (16.7 wt%) and the lowest solids yield of 30.8 wt% was achieved at 180 °C for 60 mins (SR3). All reaction conditions exceeded 40% theoretical levulinic acid yield for the evaluation of reaction temperature and reaction time on SR properties for anaerobic digestion supplementation. The aqueous phase was analysed using an HP 1100 HPLC with a BioRad Aminex 87X-H column maintained at 50 °C coupled to Refractive Index Detector (RID).

### 2.3. Characterisation of solid residues

The moisture content was measured by heating the sample in a muffle furnace at 105 °C for 24 h according to ASTM D4442. Ash content was measured by heating the sample at 550 °C for 6 h in a carbolite furnace and derived on a dry weight basis according to NREL 42622. The pH and Electrical Conductivity (EC) of the SR in deionised water was determined at 25 °C, at a solid-to-water ratio of 1:20. The CHNSO elemental combustion was carried out using an Elemental Vario El Cube analyser, with oxygen % calculated by difference according to ASTM D5291. Fixed Carbon was determined as the remaining solids on heating for 7 min at 900 °C, excluding ash content according to European Standard CEN/TS 15148:2005. Thermal Gravimetric Analysis (TGA) was conducted using a TA Instrument SDT Q50 at 10 °C/min to 900 °C in a nitrogen atmosphere. Surface Electron Microscopy (SEM) was conducted to evaluate surface and morphology of the different SRs, using a Supra 40VP-FEG Surface Electron Microscope under a partial pressure. The surface elemental composition was evaluated through Energy-Dispersive X-ray spectroscopy (EDX) utilising an AMETEK EDAX TSL.

**Table 2**

Reaction conditions for solid residue production and associated LA Yields.

Sample I.D.	Reaction Conditions		Product Yields		
	Time (mins)	Temperature (°C)	LA Yield (Theoretical)	LA Yield (wt%)	Solid Residue Yield (wt %)
SR 1	30	180	48.6%	12.6%	34.4%
SR 2	30	190	56.4%	14.6%	34.2%
SR 3	60	180	64.5%	16.7%	30.8%
SR 4	120	170	47.1%	12.2%	42.9%
SR 5	120	180	59.1%	15.3%	32.1%

The surface areas were determined by the BET method from nitrogen adsorption data at  $-196^{\circ}\text{C}$  measured with a Micromeritics ASAP2020 instrument. The samples were degassed at  $150^{\circ}\text{C}$  for 12 h prior to analysis, while the surface functional groups of the SR were characterised by FTIR spectroscopy (Spectrum Two, Perkin-Elmer, USA).

#### 2.4. Anaerobic digestion experimental design and set up

The total volatile solids (VS) of CM and inoculum was set at 8 wt% with a C/N ratio of 7.1. The SR was not included in the total VS calculations, due to the slow microbial degradation of chars according to [29]. The summary of the experimental design is shown in Table 3, which had the objective to determine the optimum SR concentration and the effect of acid hydrolysis operating conditions on SR addition to the AD of nitrogen rich feedstock (CM). The loading values of added SR have been selected based on work by Xu et al., 2018 [30], and correspond to a SR addition of 2.5 – 11.0% of TS. Since SR3 corresponded with the best acid hydrolysis conditions with regards to LA production, it was thus selected for the appraisal of the optimum SR concentration in the AD reactors in Trial 1. Trial 2 aimed instead at the investigation of different SR types, and used the experimentally determined optimum concentration of 6 g/L, identified in Trial 1.

All batch Biochemical Methane Potential (BMP) assays were conducted in 500 mL glass flasks with working volume of 200 mL. The bioreactors were sealed using ground glass joints connected to aluminium foil biogas bags, which were purged with nitrogen gas for 5 min to achieve anaerobic conditions [NO PRINTED FORM]. The batch reactors maintained at  $31 \pm 1^{\circ}\text{C}$  inside a water bath for 14 days in duplicate and manually shaken once a day. Each trial included double replicated control reactors to evaluate the inoculum biogas contribution. The biogas was measured daily and the primary biogas components,  $\text{CH}_4$  and  $\text{CO}_2$ , were analysed utilising a GeoTech 2000 biogas analyser. The biogas volumes were then converted to standard gas conditions of  $0^{\circ}\text{C}$  and 1 atm. The experimental data was fitted to a modified Gompertz equation by Gibson et al., 1987 (shown in Eq. 1) [31], using non-linear regression analysis in Matlab©(2016a). Where,  $V_{\text{CH}_4}(t)$ , is the predicted cumulative methane production (mL/g VS) at any time  $t$  (day),  $A_{\text{max}}$  is the measured cumulative methane yield (mL/g VS),  $R_{\text{max}}$  is the maximum methane production rate (mL/g VS-d),  $e$  is the mathematical constant 2.718282, and  $\lambda$  is the lag phase delay (day).

$$V_{\text{CH}_4}(t) = A_{\text{max}} \exp \left[ - \exp \left( \frac{R_{\text{max}} * e}{A_{\text{max}}} (\lambda - t) + 1 \right) \right] \quad (1)$$

#### 2.5. Monitoring of pH and ammonium

After the 14-day digestion the reactor pHs were measured using a Hanna Instruments PH211. The ammonium concentration was measured using Ion-Chromatography with a Thermo Scientific ICS5000 using suppressed conductivity detection coupled with a Dionex IonPac

**Table 3**  
Experimental design of BMP fermentation test and reactors setup.

	Reaction Conditions	Hydrochar Type	Hydrochar Concentration (g /L)
Trial 1- Effects of Solid Concentration	Control	None	None
	C1	SR 3	2
	C2	SR 3	4
	C3	SR 3	6
	C4	SR 3	8
	C5	SR 3	10
Trial 2- Effects of Different SR	Control	None	None
	D1	SR 1	6
	D2	SR 2	6
	D3	SR 3	6
	D4	SR 4	6
	D5	SR 5	6

**Table 4**

Physico-chemical characterisation of raw uncatalyzed Miscanthus and its post-reaction solid residues (SR).

Biomass Type	Miscanthus	SR 1	SR 2	SR 3	SR 4	SR 5
Ash (wt%)	2.9%	2.19%	2.64%	2.63%	2.08%	1.85%
Volatile Matter (wt%)	84.7%	68.2%	53.6%	64.2%	72.5%	65.2%
Fixed Carbon (wt %)	9.6%	26.4%	40.4%	28.3%	22.2%	29.6%
pH	3.56	2.79	2.54	2.5	2.43	2.32
EC (mS/cm)	5.48	1.71	3.36	3.14	4.28	11.68
BET (m <sup>2</sup> / g)	/	17	21	19	9	35
Bulk Atomic O/C	0.66	0.35	0.27	0.29	0.38	0.26
Surface Atomic O/C	0.72	0.41	0.40	0.50	0.38	0.54

CS16 column.

#### 2.6. Microbial community analysis

##### 2.6.1. Microbial quantification

DNA was extracted from 1 g of sample using the Quick-DNA Fecal/Soil Microbe Miniprep Kit (Zymo Research, Irvine, CA, USA) following the manufacturer's instructions. Abundance of prokaryotic cells was determined by quantitative PCR (qPCR) using SensiFAST SYBR Green Lo-ROX Mix and the MX3000P qPCR System (Agilent Genomics, Headquarters, Santa Clara, CA, United States) using universal 16 S primers [32] (forward primer and reverse primer both at 25  $\mu\text{M}$ ) [32,33]. Serial dilutions of template DNA (obtained from *Escherichia coli*, NTCT 50167) was used to construct a standard curve ranged from  $9.4 \times 10^3$  to  $9.4 \times 10^8$  cells  $\text{mL}^{-1}$  ( $5.28 \times 10^{-1}$  to  $5.28 \times 10^{-7}$  ng DNA  $\text{mL}^{-1}$ ), and meltcurve analysis corroborated the presence of a single gene-specific peak. The absolute quantification of the target genes was calculated by the standard-curve (SC) method [34].

##### 2.6.2. Microbial composition analysis

Microbial composition was profiled by sequencing the V4 region of the 16 S rRNA gene, with amplification using duplicate PCR and primers 515 F and 806 R, on a MiSeq platform (Illumina, San Diego, CA, United States), using the dual indexing method [35]. Click or tap here to enter text. Raw amplicon sequencing data were processed using the DADA2 pipeline to create amplicon sequence variants (ASVs) present in each sample [36]. Sequences below 220 bp in length and an average quality score below 30 on a window of 20 bases were discarded. Taxonomy of the ASVs was assigned using a Naive-Bayes approach implemented in the SILVA database [37].

#### 2.7. Statistical analysis

Experimental bioreactors were run simultaneously in triplicate and values given as means  $\pm$  1 standard deviation throughout. All statistical analysis were conducted using parametric tests after visual confirmation that the models conformed to the assumptions, unless otherwise stated in the text. Multivariate models were undertaken using nonmetric multidimensional scaling (NMDS) to separate out microbial communities based on their composition. Differences between the samples were assessed using permutation ANOVA (999 permutations). All diversity metrics ( $\alpha$  &  $\beta$ ) were calculated, and analysis performed in R (R Core Team, 2017) using the package vegan [38,39].

### 3. Results and discussion

#### 3.1. Solid residue characterisation for AD suitability

The thermogravimetric (TGA) and differential thermogravimetric (DTG) analysis of the five solid residue (SRs) from the acid hydrolysis

process are shown in Fig. 1. The initial mass loss can be primarily associated to the loss of residual water. The peaks at 200–300 °C on the DTG plot represent the degradation of sugars. In particular, the broad peaks in this region for SR1 and SR4 indicate incomplete hydrolysis of the cellulose, due to the milder reaction conditions of 180 °C for 30 mins and 170 °C for 120 mins respectively. This is especially evident from the low surface area value of 9 m<sup>2</sup>/g of SR4, suggesting some cellulose structures remained intact, due to the low reaction temperature of 170 °C. The incomplete hydrolysis of SR4 can be further observed in the van Krevelen plot (Figure S1), which also shows the primary SR underwent dehydration reactions, as also seen by [40]. The incomplete hydrolysis of SR4 will result in intermediate biomass-hydrochar properties that can be used as control to compare the effect of the relative effect of surface properties. SR 1, 2 and 3 exhibit higher surface area of 17–21 m<sup>2</sup>/g indicating degradation of the cellulose matrix, leaving the unreacted lignin. SR5 (180 °C, 120 mins) has a surface area of 35 m<sup>2</sup>/g, which is significantly higher than SRs produced in shorter time periods. This represents an opposite trend associated with HTC, which has noted a decrease in hydrochar surface area [41,42]. The SEM images (Figure S2) show significant carbon spheres growth on the surface of the material, which would be responsible for increased surface areas. Carbon sphere formation during acid hydrolysis has been attributed the polymerisation of reactive intermediates from sugar decomposition towards humins [9,10]. The presence of sulphuric acid catalyst may accelerate the formation of carbon spheres compared with HTC and will significantly alter the surface properties of the char. The elemental surface composition of carbonaceous spheres was estimated using EDX (Table S1), which shows surface O/C ratio varied between 0.41 and 0.54, see Table 2. The surface O/C differed with the bulk O/C ratio determined by combustion analysis (0.26–0.38), indicating that the outer surface area is rich in oxygenated functional groups. The surface functional groups were not characterised in detail however, it can be inferred that the increased O/C will increase the SR hydrophilicity and cationic exchange capacity [43,44]. This may suggest that SR 3 & 5 have increased ammonium cation absorption capacity, which is further discussed in Section 3.4. SR2 exhibited a lower O/C ratio and high fixed carbon content, possibly due to the higher degree of aromatisation caused by the higher reaction temperature. A higher degree of aromatisation is further suggested by FTIR spectroscopy (Figure S3) with the

more pronounced peaks at 1510 & 1595 cm<sup>-1</sup> associated with aromatic C=C bonds. Aromatic deoxygenated surface properties have been previously been found to have hydrophobic properties [45], which promote biofilm formation and stimulate microbial activity.

Conductive carbon materials have been proposed to promote direct interspecies electron transfer in methanogens [46], however Viggi et al. [47] suggested that bulk Electrical Conductivity (EC) is only one of many indicators of char electron transfer capacity. SR5 exhibited a remarkable EC of 11.7 mS in water compared with SR 1–4, which has been attributed to high carbon content (66.7 wt%) with possible graphitic and crystalline humin structures of the carbon spheres [41]. An increase in interspecies electron transfer can be observed as increase in biogas quality, due to the promotion of more efficient conversion of organic acids to methane relative to CO<sub>2</sub> [22]. However, it should be noted that SRs 1–4 exhibited lower electrical conductivity than that of the untreated *Miscanthus* feedstock. This is could be caused by the significant reduction of metal ions (Supplementary Table 2), due to acid leaching and it is further evidenced by the lower ash contents (range of 1.85–2.64%). This contrasts with hydrochars which generally exhibit higher ash contents than the starting feedstocks [48]. Previous studies have proposed that the hydrochars increase the bioavailability of trace elements, which have been partially attributed to promote methanogen enzymatic activity and increased methane yields [49]. The low trace element composition of the SR compared with the feedstock makes this unlikely to increase bio-availability and it can be assumed that the potential benefits of SR additives in this study would be confined to biofilm promoted microbial diversity and absorption of cation inhibitors.

### 3.2. Effects of solid residue addition on methane production (Trial 1)

The acid hydrolysis parameters (shown in Table 2) were investigated with a focus on LA production and the highest yield of 17.1 wt% (64.5% theoretical) was achieved for operating conditions leading to SR3 type residue. Therefore, SR3 (hereafter referred to as SR) was selected as additive to study the AD (methane yields were measured daily for 14 days) of the feedstock (CM), using increasing additive levels (2–10 g/L) that were loaded at the start of the digestion period. The cumulative methane yields over the 14 days are shown in Fig. 2, alongside the predicted methane yields according to the Gompertz model (Eq. (1)).

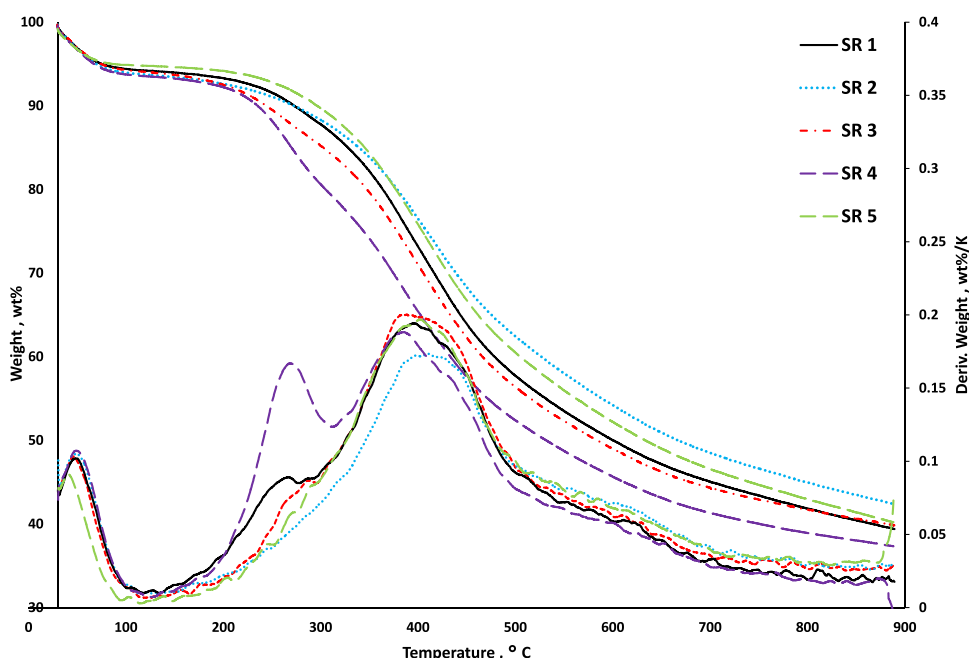


Fig. 1. : TGA and DTG curves of SR samples showing samples weight reduction with rising temperature.



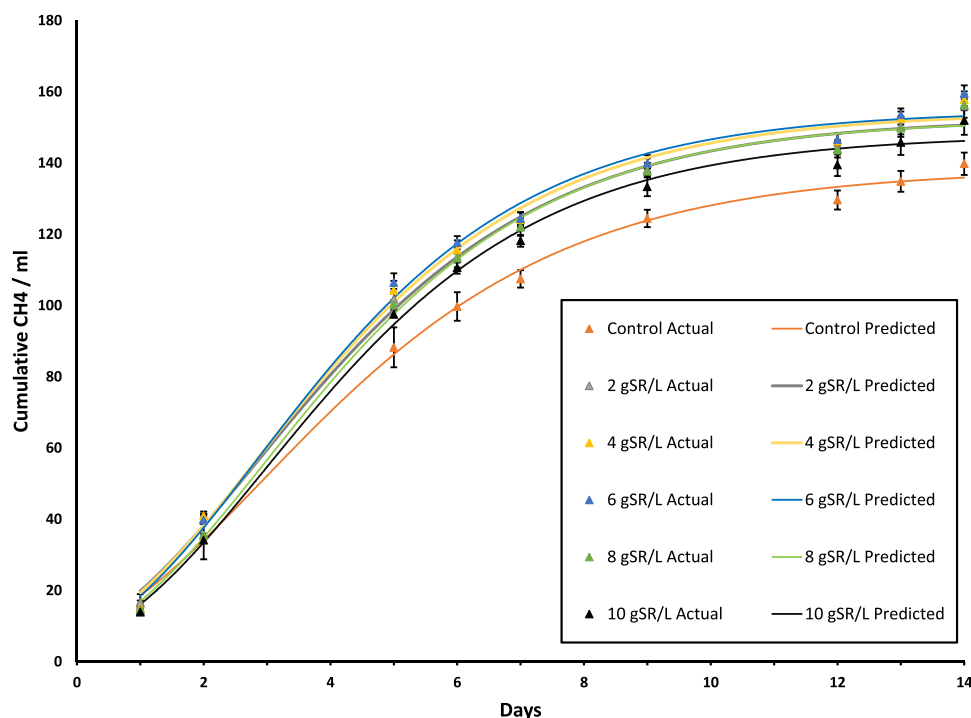


Fig. 2. : Cumulative methane yield at different SR addition against predicted yields.

The Gompertz model was statistically significant, and the calculated Gompertz model parameters are shown in Table 5. The SR addition did not stop the anaerobic digestion of CM and all reactors normally produced methane-containing biogas. The CM control yielded 136 mL CH<sub>4</sub>/gVS compared with a stoichiometric CH<sub>4</sub> potential of 459 mL/gVS and resulted in a biodegradability index of 30%. The addition of 2 gSR/L significantly increased the cumulative methane yield (+12% CH<sub>4</sub>) with respect to the CM control, strongly indicating a beneficial effect to AD, with a further minor improvement (+14.1% CH<sub>4</sub>) at 6 g/L. Increasing the SR concentration by a factor of 3 did not lead to a significant increase in CH<sub>4</sub> production, suggesting the additive is not being degraded in the reactors however, it is promoting microbial growth and absorbing inhibitors. Furthermore, the small change in methane yields (~2%) between 2 and 6 gSR/L indicates that overall the AD system is not undergoing significant stress and SR addition could potentially be more beneficial in more toxic environments. This results in lower methane yield improvements with comparable works with similar works with hydrochar and biochar that achieved improvements of +38% and +69% respectively [19,50].

A noticeable decrease in CH<sub>4</sub> yields occurred at higher SR loads (8 and 10 gSR/L), despite remaining significantly above the CM control. At

higher concentrations, chars have been reported to inhibit microbial communities [51]. This could be associated with the SR's acidic properties causing AD acidification [18] or to a minor extent as well as the presence of organic inhibitors [52] on the SR surface that were formed during the acid hydrolysis process, such as organic compounds or sulphates. Although the high sulphur content of the inoculum used in this study would suggest microbial acclimation to sulphate groups, sulphur inhibition cannot be discarded based solely on BMP yields.

The Gompertz model has successfully been used to model BMP experiments from a range of substrates [18,53]. The models' regression values in this study were all greater than 0.99 for all experimental conditions, indicating an outstanding fit of the predictive model. SR additive increased the maximum methane production ( $A_{max}$ ) achievable by 6.9–11.8% and the maximum methane production rate ( $R_{max}$ ) by 18.3–25.9%, both compared with the control reactor. This shows that SR not only increases the absolute methane yields from CM over the digestion period but also increases the maximum methane production rate. The Gompertz model parameters show that higher SR concentrations also prolonged the lag phase compared with the CM control from 0.17 days to 0.49 days. This shows that the SR slowed the microbial activity, however a lag time < 1 day indicates a high initial microbial activity and overall microbial acclimation to the system conditions. The increase in lag time for 8–10 gSR/L implies a mild inhibition taking place and that the microbial community reacted negatively to those SR levels. This can be further seen with a decrease in  $A_{max}$  from 17.15 to 16.46 mL CH<sub>4</sub>/gVS day between 6 g/L and 8 g/L, suggesting that inhibition is caused by the hydrochar itself and not from long term imbalances in the complex system.

### 3.3. Effect of different SRs on anaerobic digestion

Most of the five SRs investigated in this study resulted in higher methane yields from the anaerobic digestion of CM with 6 g/L SR concentration, as shown in Fig. 3. The highest cumulative methane yield was observed with the addition of SR3 followed by SR5, SR4 and SR1, as shown in Table 6 alongside the Gompertz model parameters. SR3 improved the cumulative methane yield relative to the un-supplemented

**Table 5**  
Summary of Kinetic data for the AD of CM at rising SR concentrations.

Condition	Cumulative CH <sub>4</sub> Yield	Modified Gompertz parameter			Statistics	
		$A_{max}$	$R_{max}$	$\lambda$	$R^2$	$p$
Control	140	138.4	18.44	0.1696	0.9960	0.9976
2 g/L	156	152.7	21.7	0.256	0.9946	0.9966
4 g/L	158	154.4	22.51	0.3189	0.9937	0.9942
6 g/L	160	154.8	23.22	0.3974	0.9917	0.9939
8 g/L	157	152.4	22.32	0.4615	0.9949	0.9960
10 g/L	152	148	21.81	0.492	0.9945	0.9963

$F$  is the measured cumulative methane production, mL/g VS added,  $A_{max}$  is the predicted cumulative methane production, mL/g VS added day,  $R_{max}$  is the maximum methane production rate, mL/g VS day, and  $\lambda$  is the duration of the lag phase.

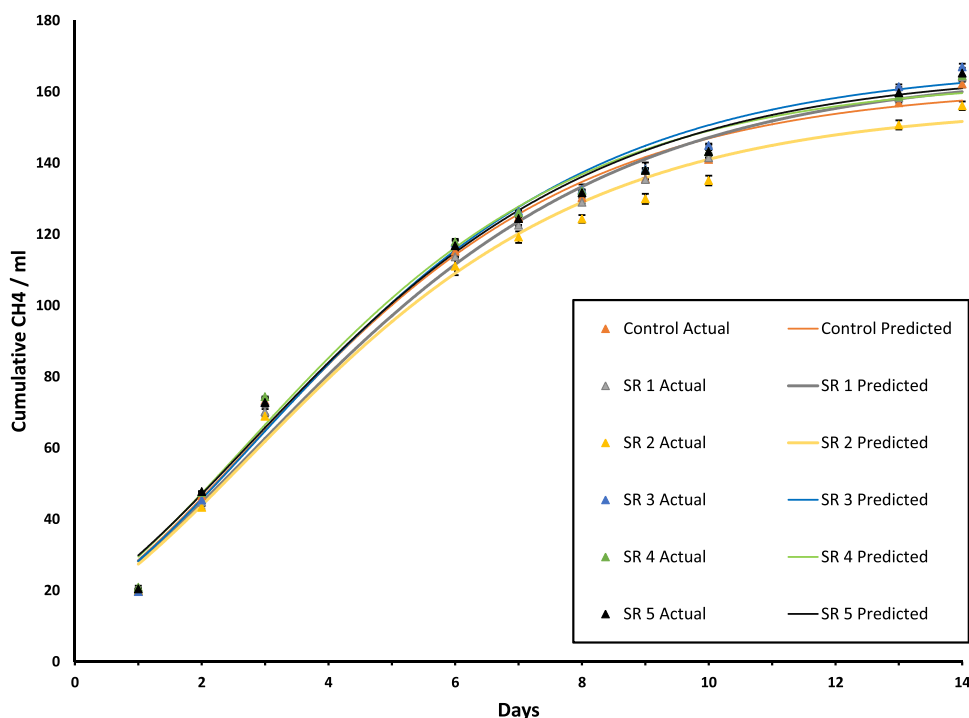


Fig. 3. : Cumulative methane yield of SRs formed under different reaction conditions.

Table 6

Summary of Kinetic data for the AD of CM with SR formed under different reaction conditions.

Condition	Cumulative CH <sub>4</sub> Yield		Modified Gompertz parameter			Statistics	
	<i>F</i>	Change due to SR	<i>A</i> <sub>Max</sub>	<i>R</i> <sup>Max</sup>	<i>λ</i>	<i>R</i> <sup>2</sup>	<i>p</i>
Control	163.5	0.0%	162	19.1	-0.40	0.9958	0.9962
SR 1	165.5	1.2%	166	18.2	-0.43	0.9932	0.9953
SR 2	157.4	-3.7%	156	18.1	-0.41	0.9949	0.9963
SR 3	168.4	3.1%	168	19.3	-0.35	0.9937	0.9966
SR 4	165.9	1.5%	164	19.4	-0.43	0.9917	0.9935
SR 5	166.6	1.9%	166	18.8	-0.49	0.9970	0.9972

*F* is the measured cumulative methane production, mL/g VS added, *A*<sub>max</sub> is the predicted cumulative methane production, mL/g VS added day, *R*<sub>Max</sub> is the maximum methane production rate, mL/ g VS day, and *λ* is the duration of the lag phase

(control) digester, by + 3.1%, which was less than 14.1% observed in Trial 1. Both trials utilised the same conditions though there were significant changes in the inoculum digester source (supplied) in terms of initial composition and microbial diversity, as shown in Section 3.5. This change was most evident in the increase in biodegradability index between Trial 1 and 2, from 30% to 35%. This suggests that the addition of SR has less effect on AD systems with higher biodegradability. It may be relevant in future to assess hydrochar addition to anaerobic digestion relative to the overall systems to accurately gauge the effects.

The SR3 was produced as the solid product from the 2 M H<sub>2</sub>SO<sub>4</sub> catalysis of *Miscanthus x Giganteus* under 180 °C for 30 mins, which not only corresponded with the highest LA yield (17.1 wt%) but also to the best methane yield improvement (3.1%). This natural synergy may suggest that more extreme catalysis conditions produce AD inhibitors such as humins. This inhibition was observed from SR2 (190 °C 30 mins), the highest reaction temperature, which was the only SR type leading to a negative effect on the methane yields. SR2 was noted as being highly carbonaceous with the highest fixed carbon content, lowest bulk O/C ratio and high aromaticity indicated by the FTIR analysis. Higher reaction temperatures may be the direct cause of this toxicity and not the humins directly, as SR5 had the most observed humin formation but did not impede the AD process. Due to the similarity in methane yields between the different SRs it is difficult to assess directly each

material property, however it does indicate that a wide variety of SRs can be used as an AD supplement. Future work should investigate the cause of the inhibitory effect and the long-term effects in AD systems in continuous feeding, with the opportunity to adapt acid hydrolysis variables to target minimised inhibition.

### 3.4. Ammonium content

The addition of even a small amount of the SR significantly decreased the ammonium contents of the reactors at the end of the digestion period, as shown in Table 7. In Trial 1, the un-supplemented control

Table 7

Ammonium content and pH of reactors after 14 days of digestion.

Trial 1			Trial 2		
Condition	Ammonium g/L	pH	Condition	Ammonium g/L	pH
Control	3.0 ± 0.2	7.62	Control	2.3 ± 0.1	8.00
2 g/L	2.3 ± 0.3	7.57	SR 1	2.0 ± 0.0	7.77
4 g/L	2.0 ± 0.1	7.56	SR 2	1.9 ± 0.1	7.69
6 g/L	2.4 ± 0.2	7.57	SR 3	2.1 ± 0.1	7.76
8 g/L	2.2 ± 0.1	7.58	SR 4	2.1 ± 0.1	7.74
10 g/L	1.9 ± 0.3	7.56	SR 5	2.1 ± 0.0	7.83

reactor with CM had an ammonium content exceeding 3 g/L, which strongly indicates ammonium inhibition associated with the digestion of nitrogen rich CM. The addition of SR decreased the ammonium concentration under all conditions, indicating partial absorbance of the ammonium. In Trial 1, increasing the SR concentration from 2 g/L to 8 g/L had negligible effect on the ammonium content indicating that SR absorbed the excess ammonium without disturbing the ammonia/ammonium buffered state. Trial 2, which investigates the different SR types, had a far lower ammonium concentration (2.3 g/L) in the control reactor, which was attributed to changes in the inoculum composition, although the addition of SR did result in decreasing ammonium concentrations being detected. The addition of SR2 caused the lowest observed ammonium concentration, 1.9 g/L, which could be attributed to absorption capacity caused by high aromaticity due to the higher formation temperature of 190 °C. However all 5 SRs were broadly similar, with values in the range of 1.9–2.1 g/L compared with the control reactor of 2.3 g/L and 1.9–2.4 g/L in Trial 1. Across both trials the SR reduced to ammonium concentrations to ~2 g/L with suggesting that an equilibrium was formed at this level. It is not clear if the decrease ammonium concentration was the only direct effect of the increased methane yields associated with the SR addition, however this shows a possible mechanism of action. Usman et al. [54] found that wood-derived hydrochar only improved methane yields by +10% at ammonium concentrations below 4 g/L which shows that under directly comparable AD conditions the SR compares favourably to other hydrochars.

### 3.5. Effect of hydrochars on microbial composition

#### 3.5.1. Effect of loading dose (Trial 1)

The effect of the varying addition of SR3 to the AD of CM was investigated for the correlation between methane yield and microbial community composition. The presence of SRs significantly altered the abundance of microbial cells ( $F_{4,5} = 10.5$ ,  $p = 0.006$ ; Table 8). Further, significant effects with increased loading of hydrochars ( $F_{4,5} = 7.32$ ,  $p = 0.025$ ) were observed. Here, increasing hydrochar load broadly correlated to increasing microbial cell count. Our analysis also indicated that the microbial diversity at the domain level was dominated by bacteria in all the samples ( $97.5 \pm 0.7\%$ ). Organisms belonging to domain bacteria were significantly more abundant on the SR samples than the inoculum ( $F_{5,6} = 11$ ,  $p = 0.005$ ). This result meant that there was a lower abundance of archaea in the SR samples ( $2.5 \pm 0.7\%$ ). Microbial communities were dominated by phyla Bacteroidetes ( $43.2 \pm 1.1\%$ ) and Firmicutes ( $38.5 \pm 2.1\%$ ). Differences in microbial composition were visualised on NMDS ordination space and the presence of SRs significantly (PERMANOVA  $F_{1,11} = 37.14$ ,  $p = 0.016$ ,  $R^2 = 0.79$ ) altered the composition of the communities and this change was strongly correlated ( $R^2 = 0.99$ ,  $t_{10} = 22.825$ ,  $p < 0.001$ ) with an increase in methane yield (Fig. 4).

#### 3.5.2. Effect of different hydrochars (Trial 2)

Samples treated with different substrates (SR1 to SR5) ranged between  $2.51 \times 10^{11}$  to  $6.09 \times 10^{11}$  cells mL<sup>-1</sup> ( $3.86 \times 10^{11} \pm 1.3 \times 10^{11}$  cells mL<sup>-1</sup>). The addition of different SRs significantly ( $F_{4,5} = 8.37$ ,  $p = 0.010$ ) altered (Table 8) the abundance of microorganisms. Further

**Table 8**

Post-digestion cells count results from quantitative PCR for all SRs conditions.

Trial 1		Trial 2	
Condition	Cells per mL	Condition	Cells per mL
Control	1.46E+11	Control	5.08E+11
SR3 2 g/L	2.13E+11	SR 1	5.23E+11
SR3 4 g/L	1.84E+11	SR 2	6.02E+11
SR3 6 g/L	1.16E+11	SR 3	1.93E+11
SR3 8 g/L	2.87E+11	SR 4	2.84E+11
SR3 10 g/L	2.92E+11	SR 5	3.15E+11

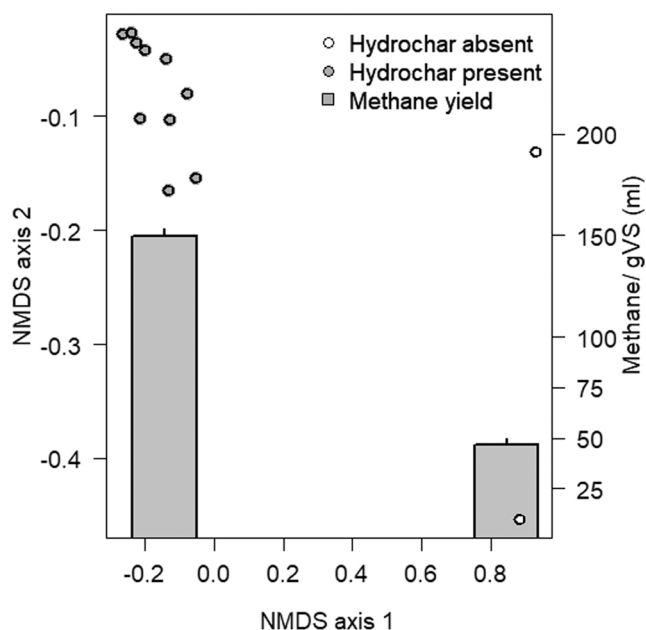


**Fig. 4.** : NMDS graph of microbial composition alongside methane yield from Trial 1, showing changes in microbial composition are correlated with increased methane yield. The SRs were also found to cause significant dissimilarities between the inoculum and SR samples (b, circles), which was also found to correlate with an increased methane yield (bars).

differences ( $F_{4,5} = 6.31$ ,  $p = 0.030$ ) were observed between the different SRs used. Most notably, SR3 had the lowest observed microbial cell count relative to the other SRs in Trial 2, despite having the highest methane yields. While SR2 which had a negative effect on the methane yields had the highest observed microbial cell count. This indicates that the effect of SR is not directly linked to microbial abundance and suggests that the SRs properties have differing effects on the complex microbial communities.

The alpha diversity (observed, Chao1, Simpson and Shannon indices) was consistent among the samples, and no significant differences were detected by ANOVA across the hydrochar samples (Table S4). There was no change in the dominant microorganisms between this and the previous experiment where organisms affiliated to Bacteroidetes ( $40.9 \pm 1.55\%$ ) and Firmicutes ( $39.1 \pm 2\%$ ) were the most prevalent. Organisms affiliated to phyla Bacteroidetes and Firmicutes have been reported as the main microbial components in similar anaerobic digestion processes, and main bacteria impacting the methane yield, shown in Fig. 5 [55,56]. Regarding archaeal organisms, phylum Halobacteriota includes hydrogenotrophic, acetate/H<sub>2</sub>/formate oxidizing, methanogenic, hydrocarbon utilizing groups (order/genus), and its presence has frequently been detected on refinery waste environments [57]. Interestingly, in this study the methanogenic *Methanosaeta* increased to dominate the bioreactors, although this was not statistically significant (one-sample Wilcoxon rank sum test  $V = 15$ ,  $p = 0.065$ ), resulted in the methanogenesis being almost entirely produced via an acetate precursor [58]. The cumulative yield of methane detected on this project corroborates that the syntrophic interaction between bacterial and archaeal organisms (established by acidogenesis and methanogenesis) occurs within the AD system [59].

Additionally, the production of methane may be occurring through other processes such as direct interspecies electron transfer (DIET) [60, 61]. The results above show that the relative abundance of Archaea decreased significantly (one-sample Wilcoxon rank sum test  $V = 0$ ,  $p = 0.002$ ) in the presence of the hydrochar substrates ( $2.10 \pm 0.67\%$ , SR3 2–10 g/L and SR1 to SR5) compared to inoculum control ( $19.62\%$ ). However, the high methane yields may indicate that the lower relative abundances did not mean the lower absolute concentrations of



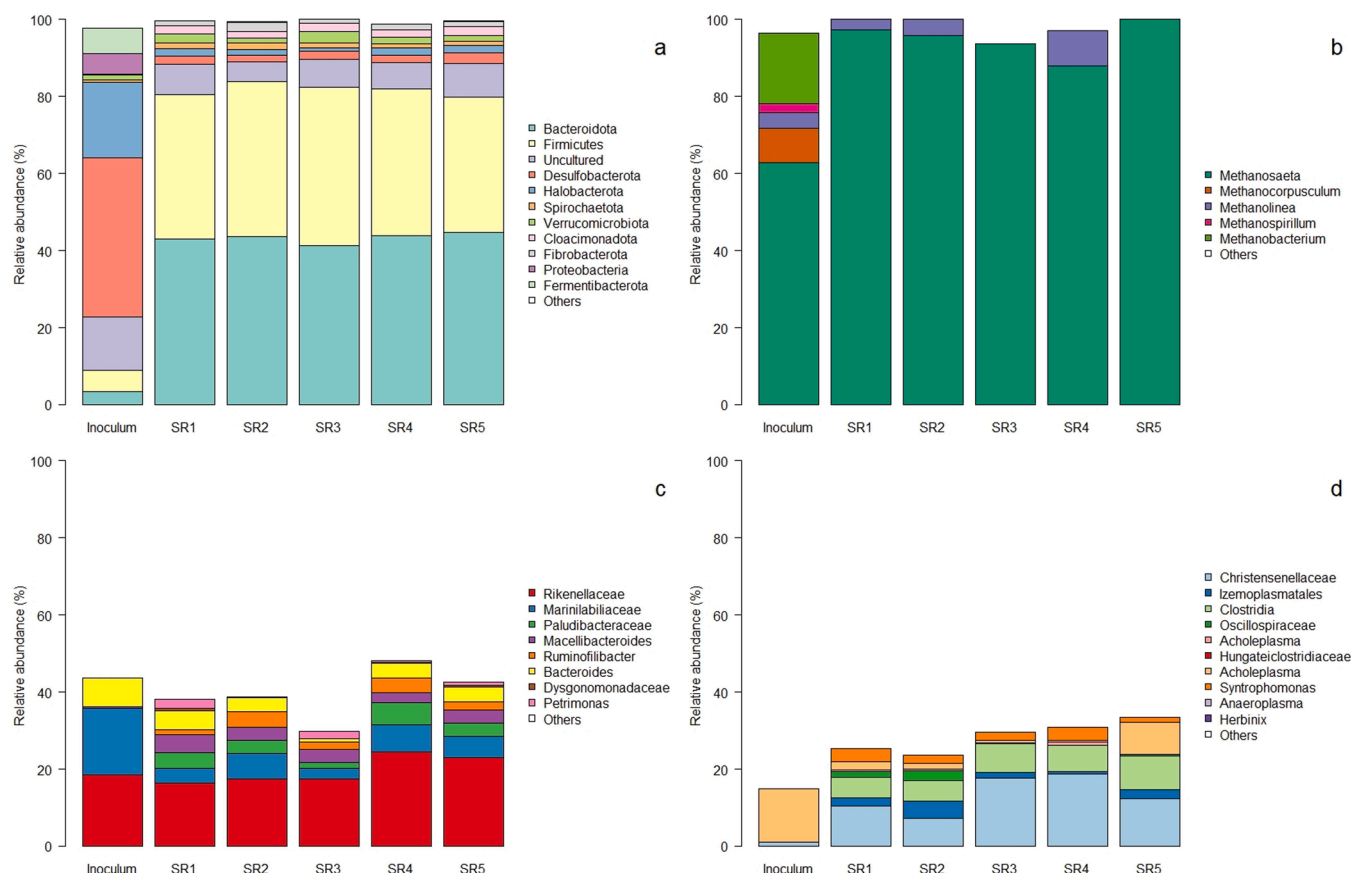


Fig. 5. : Relative microbial composition during Trial 2 at a) genera, b) methanogens, c) bacteroides, and d) firmicutes levels.

methanogens archaea [62]. In addition, results suggest that the archaeal community is becoming more specialized towards using the substrate to produce methane, a phenomenon observed in similar anaerobic digestion processes [63]. Another possible explanation for the decrease of the methanogens is the stability of the AD system since it has been reported that archaeal methanogens are more often observed in extreme conditions due to their higher robustness [64]. Interestingly, SR2 which negatively impacted the 14-day methane yields compared with the control reactor had minimal differences in microbial composition compared with the other SRs. This shows that the SR2 still exhibited microbial promotion properties. This indicates that the microbial inhibitors formed during the high temperature catalysis (190 °C) were likely metabolic inhibitors, which corresponds with the abnormally high microbial cell count.

Our results show that whilst the presence of hydrochar has a significant effect on composition (PERMANOVA  $F_{1,9}=70.02$ ,  $p=0.010$ ,  $R^2=0.88$ ), however, once this is accounted for, there is no difference between the microbial composition and either the amount of hydrochar loaded ( $F_{1,9}=0.38$ ,  $p=0.597$ ,  $R^2=0.01$ ) or methane yield ( $R^2=0.11$ ,  $t_8=0.31$ ,  $p=0.767$ ). Therefore, the addition of a small quantity of SR formed under any conditions was sufficient to induce microbial change towards a more diverse equilibrium condition. The microbial promotion activity of solid residues could be caused by either the functionalised microporous structures or due to the associated reduction in ammonium concentrations.

#### 4. Conclusion

In this work, the application of SR from the acid catalysed production of LA from lignocellulosic biomass was evaluated with regards to solid properties, methane potential, residue concentration, effect on

ammonium concentration and microbial composition. The conclusions are as follows:

- SR from acid hydrolysis of lignocellulosic biomass could be used as an anaerobic digestion supplement under a wide range of conditions
- The SR produced at the optimum LA conditions resulted in a + 14% increase in methane yields compared with the control reactor with an optimised concentration of 6 g/L
- SR reduced ammonium concentration and increased microbial diversity under all conditions analysed
- The SR produced from the highest yielding LA catalysis conditions (64.5%), 180 °C for 60 min, suggesting possible inherent synergies between catalysis and hydrochar optimisation as a balance between surface functionalisation and inhibitor formation
- The application of waste solid residue from biorefineries could potentially be used as a low-cost char substance for the improvement of a large variety of difficult AD feedstocks.

#### CRedit authorship contribution statement

**George Hurst:** Conceptualization, Investigation, Formal analysis, Writing – original draft, Visualization. **Sharon Ruiz-Lopez:** Investigation, Methodology, Formal analysis, Writing – review & editing. **Damian Rivett:** Investigation, Methodology, Formal analysis, Writing – review & editing, Visualization. **Silvia Tedesco:** Methodology, Formal analysis, Writing – review & editing, Supervision, Project administration.

#### Declaration of Competing Interest

The authors declare that they have no known competing financial

interests or personal relationships that could have appeared to influence the work reported in this paper.

## Data availability

Data will be made available on request.

## Acknowledgements

This research was supported by Manchester Metropolitan University via the Research Accelerator Grants (RAG) and the Strategic Opportunities Fund awarded (SOF) awarded to Dr Tedesco and Dr Rivett respectively. The authors would also like to thank Dr Tosheva for kindly performing BET analysis of the solid residues.

## Appendix A. Supporting information

Supplementary data associated with this article can be found in the online version at [doi:10.1016/j.jece.2022.108343](https://doi.org/10.1016/j.jece.2022.108343).

## References

- [1] A. Mukherjee, M.J. Dumont, V. Raghavan, Review: Sustainable production of hydroxymethylfurfural and levulinic acid: Challenges and opportunities, *Biomass Bioenergy* 72 (2015) 143–183, <https://doi.org/10.1016/j.biombioe.2014.11.007>.
- [2] G. Hurst, J.M. González-Carballo, L. Tosheva, S. Tedesco, Synergistic catalytic effect of sulphated zirconia-HCl system for levulinic acid and solid residue production using microwave irradiation, *Energ. (Basel)* 14 (2021), <https://doi.org/10.3390/en14061582>.
- [3] F.D. Pileidis, M.M. Titirici, Levulinic acid biorefineries: new challenges for efficient utilization of biomass, *ChemSusChem* 9 (2016) 562–582, <https://doi.org/10.1002/cssc.201501405>.
- [4] D.J. Hayes, F. Steve, M.H.B. Hayes, J. Ross, *The biofine process - production of levulinic acid, furfural, and formic acid from lignocellulosic feedstocks*, Wiley-VCH Verl. GmbH Wein. (2008).
- [5] M. Sajid, X. Zhao, D. Liu, Production of 2,5-furandicarboxylic acid (FDCA) from 5-hydroxymethylfurfural (HMF): Recent progress focusing on the chemical-catalytic routes, *Green. Chem.* 20 (2018) 5427–5453, <https://doi.org/10.1039/c8gc02680g>.
- [6] S. Takkellapati, T. Li, M.A. Gonzalez, An overview of biorefinery-derived platform chemicals from a cellulose and hemicellulose biorefinery, *Clean. Technol. Environ. Policy* 20 (2018) 1615–1630, <https://doi.org/10.1007/s10098-018-1568-5>.
- [7] F. Melligan, K. Dussan, R. Auccaise, E.H. Novotny, J.J. Leahy, M.H.B. Hayes, W. Kwapinski, Characterisation of the products from pyrolysis of residues after acid hydrolysis of Miscanthus, *Bioresour. Technol.* 108 (2012) 258–263, <https://doi.org/10.1016/j.biortech.2011.12.110>.
- [8] G. Hurst, I. Brangeli, M. Peeters, S. Tedesco, Solid residue and by-product yields from acid-catalysed conversion of poplar wood to levulinic acid, *Chem. Pap.* 74 (2020) 1647–1661, <https://doi.org/10.1007/s11696-019-01013-3>.
- [9] S.K.R.R. Patil, J. Heltzel, C.R.F.F. Lund, Comparison of structural features of humins formed catalytically from glucose, fructose, and 5-hydroxymethylfurfuraldehyde, *Energy Fuels* 26 (2012) 5281–5293, <https://doi.org/10.1021/ef3007454>.
- [10] I. van Zandvoort, E.J. Koers, M. Weingarth, P.C.A. Bruijninx, M. Baldus, B. M. Weckhuysen, Structural characterization of 13C-enriched humins and alkali-treated 13C humins by 2D solid-state NMR, *Green. Chem.* 17 (2015) 4383–4392, <https://doi.org/10.1039/c5gc00327j>.
- [11] E.S. Lopes, J.F. Leal Silva, E.C. Rivera, A.P. Gomes, M.S. Lopes, R. Maciel Filho, L. P. Tovar, Challenges to levulinic acid and humins valuation in the sugarcane bagasse biorefinery concept, *Bioenergy Res.* (2020), <https://doi.org/10.1007/s12155-020-10124-9>.
- [12] A. Mountraki, M. Tsakalova, A. Panteli, A.I. Papoutsis, A.C. Kokkosis, Integr. Waste Manag. Multiproduct Biorefineries: Syst. Optim. Anal. a Real. -Life Ind. Plant (2016), <https://doi.org/10.1021/acs.iecr.5b03431>.
- [13] F. Melligan, K. Dussan, R. Auccaise, E.H. Novotny, J.J. Leahy, M.H.B. Hayes, W. Kwapinski, Characterisation of the products from pyrolysis of residues after acid hydrolysis of Miscanthus, *Bioresour. Technol.* 108 (2012) 258–263, <https://doi.org/10.1016/j.biortech.2011.12.110>.
- [14] A. Mija, J.C. van der Waal, J. Pin, N. Guigo, E. de Jong, Humins as promising material for producing sustainable carbohydrate-derived building materials, *Constr. Build. Mater.* 139 (2017) 594–601, <https://doi.org/10.1016/j.conbuildmat.2016.11.019>.
- [15] L. Cao, I.K.M. Yu, D.W. Cho, D. Wang, D.C.W. Tsang, S. Zhang, S. Ding, L. Wang, Y. S. Ok, Microwave-assisted low-temperature hydrothermal treatment of red seaweed (*Gracilaria lemaneiformis*) for production of levulinic acid and algae hydrochar, *Bioresour. Technol.* 273 (2019) 251–258, <https://doi.org/10.1016/j.biortech.2018.11.013>.
- [16] J. Fang, L. Zhan, Y.S. Ok, B. Gao, Minireview of potential applications of hydrochar derived from hydrothermal carbonization of biomass, *J. Ind. Eng. Chem.* 57 (2018) 15–21, <https://doi.org/10.1016/j.jiec.2017.08.026>.
- [17] N. Shi, Q. Liu, X. He, G. Wang, N. Chen, J. Peng, L. Ma, Molecular structure and formation mechanism of hydrochar from hydrothermal carbonization of carbohydrates, *Energy Fuels* 33 (2019) 9904–9915, <https://doi.org/10.1021/acs.energyfuels.9b02174>.
- [18] J. Pan, J. Ma, X. Liu, L. Zhai, X. Ouyang, H. Liu, Effects of different types of biochar on the anaerobic digestion of chicken manure, *Bioresour. Technol.* 275 (2019) 258–265, <https://doi.org/10.1016/j.biortech.2018.12.068>.
- [19] X. Pan, Y. Zhang, C. He, G. Li, X. Ma, Q. Zhang, L. Liu, M. Lan, Y. Jiao, Enhancement of anaerobic fermentation with corn straw by pig bone-derived biochar, *Sci. Total Environ.* 829 (2022), 154326, <https://doi.org/10.1016/j.scitotenv.2022.154326>.
- [20] K. Betlem, A. Kaur, A.D. Hudson, R.D. Crapnell, G. Hurst, P. Singla, M. Zubko, S. Tedesco, C.E. Banks, K. Whitehead, M. Peeters, Heat-Transfer Method: A Thermal Analysis Technique for the Real-Time Monitoring of Staphylococcus aureus Growth in Buffered Solutions and Digestate Samples, *ACS Appl. Bio Mater.* 2 (2019) 3790–3798, <https://doi.org/10.1021/acsabm.9b00409>.
- [21] S. Tedesco, G. Hurst, A. Imtiaz, M. Ratova, L. Tosheva, P. Kelly, TiO<sub>2</sub> supported natural zeolites as biogas enhancers through photocatalytic pre-treatment of Miscanthus x giganteus crops, *Energy* 205 (2020), <https://doi.org/10.1016/j.energy.2020.117954>.
- [22] S.O. Masebinu, E.T. Akinlabi, E. Muzenda, A.O. Aboyade, A review of biochar properties and their roles in mitigating challenges with anaerobic digestion, *Renew. Sustain. Energy Rev.* 103 (2019) 291–307, <https://doi.org/10.1016/j.rser.2018.12.048>.
- [23] X. Liu, M. Du, Q. Lu, D. He, K. Song, Q. Yang, A. Duan, D. Wang, How Does Chitosan Affect Methane Production in Anaerobic Digestion, *Environ. Sci. Technol.* 55 (2021) 15843–15852, <https://doi.org/10.1021/acs.est.1c04693>.
- [24] X. Liu, Y. Wu, Q. Xu, M. Du, D. Wang, Q. Yang, G. Yang, H. Chen, T. Zeng, Y. Liu, Q. Wang, B.J. Ni, Mechanistic insights into the effect of poly ferric sulfate on anaerobic digestion of waste activated sludge, *Water Res.* 189 (2021), <https://doi.org/10.1016/j.watres.2020.116645>.
- [25] G. Hurst, M. Peeters, S. Tedesco, Integration of catalytic biofuel production and anaerobic digestion for biogas production, *Springer Int. Publ.* (2021), [https://doi.org/10.1007/978-3-030-63916-7\\_16](https://doi.org/10.1007/978-3-030-63916-7_16).
- [26] L. Qiu, Y.F. Deng, F. Wang, M. Davaritouchae, Y.Q. Yao, A review on biochar-mediated anaerobic digestion with enhanced methane recovery, *Renew. Sustain. Energy Rev.* 115 (2019), 109373, <https://doi.org/10.1016/j.rser.2019.109373>.
- [27] S. Majumder, S. Neogi, T. Dutta, M.A. Powel, P. Banik, The impact of biochar on soil carbon sequestration: Meta-analytical approach to evaluating environmental and economic advantages, *J. Environ. Manag.* 250 (2019), 109466, <https://doi.org/10.1016/j.jenvman.2019.109466>.
- [28] M. Kumar, S. Dutta, S. You, G. Luo, S. Zhang, P.L. Show, A.D. Sawarkar, L. Singh, D.C.W. Tsang, A critical review on biochar for enhancing biogas production from anaerobic digestion of food waste and sludge, *J. Clean. Prod.* 305 (2021), 127143, <https://doi.org/10.1016/j.jclepro.2021.127143>.
- [29] M. Gronwald, C. Vos, M. Helfrich, A. Don, Stability of pyrochar and hydrochar in agricultural soil - a new field incubation method, *Geoderma* 284 (2016) 85–92, <https://doi.org/10.1016/j.geoderma.2016.08.019>.
- [30] J. Xu, A.M. Mustafa, H. Lin, U.Y. Choe, K. Sheng, Effect of hydrochar on anaerobic digestion of dead pig carcass after hydrothermal pretreatment, *Waste Manag.* 78 (2018) 849–856, <https://doi.org/10.1016/j.wasman.2018.07.003>.
- [31] A.M. Gibson, N. Bratchell, T.A. Roberts, The effect of sodium chloride and temperature on the rate and extent of growth of Clostridium botulinum type A in pasteurized pork slurry, *J. Appl. Bacteriol.* 62 (1987) 479–490, <https://doi.org/10.1111/j.1365-2672.1987.tb02680.x>.
- [32] M.A. Nadkarni, F.E. Martin, N.A. Jacques, N. Hunter, Determination of bacterial load by real-time PCR using a broad-range (universal) probe and primers set, *Microbiol. (N. Y.)* 148 (2002) 257–266, <https://doi.org/10.1099/00221287-148-1-257>.
- [33] S. Ruiz-Lopez, L. Foster, C. Boothman, N. Cole, K. Morris, J.R. Lloyd, Identification of a Stable Hydrogen-Driven Microbiome in a Highly Radioactive Storage Facility on the Sellafield Site, *Front. Microbiol.* 11 (2020), <https://doi.org/10.3389/fmicb.2020.587556>.
- [34] R. Brankatschk, N. Bodenhausen, J. Zeyer, H. Burgmann, Simple absolute quantification method correcting for quantitative PCR efficiency variations for microbial community samples, *Appl. Environ. Microbiol.* 78 (2012) 4481–4489, <https://doi.org/10.1128/AEM.07878-11>.
- [35] J.J. Kozich, S.L. Westcott, N.T. Baxter, S.K. Highlander, P.D. Schloss, Development of a dual-index sequencing strategy and curation pipeline for analyzing amplicon sequence data on the miseq illumina sequencing platform, *Appl. Environ. Microbiol.* 79 (2013) 5112–5120, <https://doi.org/10.1128/AEM.01043-13>.
- [36] B.J. Callahan, P.J. McMurdie, M.J. Rosen, A.W. Han, A.J.A. Johnson, S.P. Holmes, DADA2: High resolution sample inference from Illumina amplicon data, *Nat. Methods* 13 (2016) 4–5, <https://doi.org/10.1038/nmeth.3869>.
- [37] C. Quast, E. Pruesse, P. Yilmaz, J. Gerken, T. Schweer, P. Yarza, J. Peplies, F. O. Glöckner, The SILVA ribosomal RNA gene database project: Improved data processing and web-based tools, *Nucleic Acids Res.* 41 (2013) 590–596, <https://doi.org/10.1093/nar/gks1219>.
- [38] R. Team, Development core, a language and environment for statistical computing, *R. Found. Stat. Comput.* 2 (2017), <https://www.R-project.org/>.
- [39] J. Oksanen, F.G. Blanchet, M. Friendly, R. Kindt, P. Legendre, D. Mcglinn, P. R. Minchin, R.B. O'hara, G.L. Simpson, P. Solymos, M. Henry, H. Stevens, E. Szoecs, H.W. Maintainer, Package “vegan”, Title Community Ecol. Package, *Community Ecol. Package* 2 (2019) 1–297.
- [40] I. van Zandvoort, Y. Wang, C.B. Rasrendra, E.R.H. van Eck, P.C.A. Bruijninx, H. J. Heeres, B.M. Weckhuysen, Formation, molecular structure, and morphology of

- humins in biomass conversion: Influence of feedstock and processing conditions, *ChemSusChem* 6 (2013) 1745–1758, <https://doi.org/10.1002/cssc.201300332>.
- [41] V. Hoffmann, D. Jung, J. Zimmermann, C.R. Correa, A. Elleuch, K. Halouani, A. Kruse, Conductive carbon materials from the hydrothermal carbonization of vineyard residues for the application in electrochemical double-layer capacitors (EDLCs) and direct carbon fuel cells (DCFCs), *Materials* 12 (2019), <https://doi.org/10.3390/MA12101703>.
- [42] J. Cai, B. Li, C. Chen, J. Wang, M. Zhao, K. Zhang, Hydrothermal carbonization of tobacco stalk for fuel application, *Bioresour. Technol.* 220 (2016) 305–311, <https://doi.org/10.1016/j.biortech.2016.08.098>.
- [43] F. Masís-Meléndez, D. Segura-Chavarría, C.A. García-González, J. Quesada-Kimsey, K. Villagra-Mendoza, Variability of physical and chemical properties of TLUD stove derived biochars, *Appl. Sci. (Switz.)* 10 (2020) 1–20, <https://doi.org/10.3390/app10020507>.
- [44] A. Dieguez-Alonso, A. Funke, A. Anca-Couce, A.G. Rombolà, G. Ojeda, J. Bachmann, F. Behrendt, Towards biochar and hydrochar engineering-influence of process conditions on surface physical and chemical properties, thermal stability, nutrient availability, toxicity and wettability, *Energ. (Basel)* 11 (2018), <https://doi.org/10.3390/en11030496>.
- [45] F. Masís-Meléndez, D. Segura-Chavarría, C.A. García-González, J. Quesada-Kimsey, K. Villagra-Mendoza, Variability of physical and chemical properties of TLUD stove derived biochars, *Appl. Sci. (Switz.)* 10 (2020) 1–20, <https://doi.org/10.3390/app10020507>.
- [46] W. Guo, Y. Li, K. Zhao, Q. Xu, H. Jiang, H. Zhou, Performance and microbial community analysis of anaerobic digestion of vinegar residue with adding of acetylene black or hydrochar, *Waste Biomass. Valoriz.* (2019), <https://doi.org/10.1007/s12649-019-00664-3>.
- [47] C. Cruz Viggli, S. Simonetti, E. Palma, P. Pagliaccia, C. Braguglia, S. Fazi, S. Baronti, M.A. Navarra, I. Pettiti, C. Koch, F. Harnisch, F. Aulenta, Enhancing methane production from food waste fermentate using biochar: The added value of electrochemical testing in pre-selecting the most effective type of biochar, *Biotechnol. Biofuels* 10 (2017) 1–13, <https://doi.org/10.1186/s13068-017-0994-7>.
- [48] T. Wang, Y. Zhai, Y. Zhu, C. Li, G. Zeng, A review of the hydrothermal carbonization of biomass waste for hydrochar formation: Process conditions, fundamentals, and physicochemical properties, *Renew. Sustain. Energy Rev.* 90 (2018) 223–247, <https://doi.org/10.1016/j.rser.2018.03.071>.
- [49] T.G. Ambaye, E.R. Rene, A.S. Nizami, C. Dupont, M. Vaccari, E.D. van Hullebusch, Beneficial role of biochar addition on the anaerobic digestion of food waste: A systematic and critical review of the operational parameters and mechanisms, *J. Environ. Manag.* 290 (2021), 112537, <https://doi.org/10.1016/j.jenvman.2021.112537>.
- [50] S. Ren, M. Usman, D.C.W. Tsang, S. O-Thong, I. Angelidaki, X. Zhu, S. Zhang, G. Luo, Hydrochar-Facilitated Anaerobic Digestion: Evidence for Direct Interspecies Electron Transfer Mediated through Surface Oxygen-Containing Functional Groups, *Environ. Sci. Technol.* 54 (2020) 5755–5766, <https://doi.org/10.1021/acs.est.0c00112>.
- [51] M. Dudek, K. Świechowski, P. Manczarski, J.A. Koziel, A. Białowiec, The effect of biochar addition on the biogas production kinetics from the anaerobic digestion of brewers' spent grain, *Energ. (Basel)* 12 (2019) 1–22, <https://doi.org/10.3390/en12081518>.
- [52] M. Du, X. Liu, D. Wang, Q. Yang, A. Duan, H. Chen, Y. Liu, Q. Wang, B.J. Ni, Understanding the fate and impact of capsaicin in anaerobic co-digestion of food waste and waste activated sludge, *Water Res.* 188 (2021), <https://doi.org/10.1016/j.watres.2020.116539>.
- [53] G.K. Kafle, L. Chen, Comparison on batch anaerobic digestion of five different livestock manures and prediction of biochemical methane potential (BMP) using different statistical models, *Waste Manag.* 48 (2016) 492–502, <https://doi.org/10.1016/j.wasman.2015.10.021>.
- [54] M. Usman Khan, B. Kiaer Ahring, Improving the biogas yield of manure: Effect of pretreatment on anaerobic digestion of the recalcitrant fraction of manure, *Bioresour. Technol.* 321 (2021), 124427, <https://doi.org/10.1016/j.biortech.2020.124427>.
- [55] N. Krakat, S. Schmidt, P. Scherer, Potential impact of process parameters upon the bacterial diversity in the mesophilic anaerobic digestion of beet silage, *Bioresour. Technol.* 102 (2011) 5692–5701, <https://doi.org/10.1016/j.biortech.2011.02.108>.
- [56] M. Usman, Z. Shi, S. Ren, H.H. Ngo, G. Luo, S. Zhang, Hydrochar promoted anaerobic digestion of hydrothermal liquefaction wastewater: Focusing on the organic degradation and microbial community, *Chem. Eng. J.* 399 (2020), 125766, <https://doi.org/10.1016/j.cej.2020.125766>.
- [57] J. Sarkar, S.K. Kazy, A. Gupta, A. Dutta, B. Mohapatra, A. Roy, P. Bera, A. Mitra, P. Sar, Biostimulation of indigenous microbial community for bioremediation of petroleum refinery sludge, *Front. Microbiol.* 7 (2016) 1–20, <https://doi.org/10.3389/fmicb.2016.01407>.
- [58] P.H. Janssen, Selective enrichment and purification of cultures of *Methanosaeta* spp., n.d. [www.elsevier.com/locate/jmimeth](http://www.elsevier.com/locate/jmimeth).
- [59] C.A. Bareither, G.L. Wolfe, K.D. McMahon, C.H. Benson, Microbial diversity and dynamics during methane production from municipal solid waste, *Waste Manag.* 33 (2013) 1982–1992, <https://doi.org/10.1016/j.wasman.2012.12.013>.
- [60] M. Usman, S. Hao, H. Chen, S. Ren, D.C.W. Tsang, S. O-Thong, G. Luo, S. Zhang, Molecular and microbial insights towards understanding the anaerobic digestion of the wastewater from hydrothermal liquefaction of sewage sludge facilitated by granular activated carbon (GAC), *Environ. Int.* 133 (2019), 105257, <https://doi.org/10.1016/j.envint.2019.105257>.
- [61] C.L. Hemme, Y. Deng, T.J. Gentry, M.W. Fields, L. Wu, S. Barua, K. Barry, S. G. Tringe, D.B. Watson, Z. He, T.C. Hazen, J.M. Tiedje, E.M. Rubin, J. Zhou, Metagenomic insights into evolution of a heavy metal-contaminated groundwater microbial community, *ISME J.* 4 (2010) 660–672, <https://doi.org/10.1038/ismej.2009.154>.
- [62] J. He, S. Ren, S. Zhang, G. Luo, Modification of hydrochar increased the capacity to promote anaerobic digestion, *Bioresour. Technol.* 341 (2021), 125856, <https://doi.org/10.1016/j.biortech.2021.125856>.
- [63] E.A.F. Vasconcelos, S.T. Santaella, M.B. Viana, A.B. dos Santos, G.C. Pinheiro, R. C. Leitão, Composition and ecology of bacterial and archaeal communities in anaerobic reactor fed with residual glycerol, *Anaerobe* 59 (2019) 145–153, <https://doi.org/10.1016/j.anaerobe.2019.06.014>.
- [64] H. Pasalari, M. Gholami, A. Rezaee, A. Esrafil, M. Farzadkia, Perspectives on microbial community in anaerobic digestion with emphasis on environmental parameters: A systematic review, *Chemosphere* 270 (2021), <https://doi.org/10.1016/j.chemosphere.2020.128618>.